IOPscience iopscience.iop.org

Home Search Collections Journals About Contact us My IOPscience

The response of silicon detectors to low-energy ion implantation

This article has been downloaded from IOPscience. Please scroll down to see the full text article.

2008 J. Phys.: Condens. Matter 20 415205

(http://iopscience.iop.org/0953-8984/20/41/415205)

View the table of contents for this issue, or go to the journal homepage for more

Download details:
IP Address: 129.252.86.83
The article was downloaded on 29/05/2010 at 15:35

Please note that terms and conditions apply.

J. Phys.: Condens. Matter **20** (2008) 415205 (7pp) doi:10.1088/0953-8984/20/41/415205

The response of silicon detectors to low-energy ion implantation

T Hopf[1], C Yang[1], S E Andresen[2] and D N Jamieson[1]

[1] Centre for Quantum Computer Technology, School of Physics, University of Melbourne, Victoria 3010, Australia
[2] Niels Bohr Institute, University of Copenhagen, Universitetsparken 5, 2100 København Ø, Denmark

E-mail: t.hopf@imperial.ac.uk

Received 7 August 2008, in final form 1 September 2008
Published 12 September 2008
Online at stacks.iop.org/JPhysCM/20/415205

Abstract
Studies of electrical transients in single-crystal silicon induced by discrete low-energy (sub-20 keV) ions have been carried out at 90 K, with ionization measurements and damage accumulation in the sample being investigated. Ionization studies reveal a discrepancy between experimental results and predictions from the widely used SRIM (stopping and range of ions in matter) code, one which increases with decreasing energy: a result which has previously been suggested from studies with continuous ion beams. Damage accumulation studies of the sample also demonstrate that current models of damage build-up in silicon are inadequate at such low energies, with experiments indicating that individual ions create a much larger region of decreased charge collection efficiency outside of the small amorphous cores known to be formed by such impacts.

(Some figures in this article are in colour only in the electronic version)

1. Introduction

We have recently developed a detection system for the counted implantation of single low-energy ions into silicon, based on the collection of ionization generated in the substrate by each individual ion impact [1]. The basis of this technique is a pin diode structure integrated onto a high-resistivity (∼15 kΩ cm) n-type single-crystal silicon wafer, which is operated in a reverse-bias condition in order to fully deplete the wafer (figure 1). Coupled with appropriate signal processing electronics, this detector structure allows for the low-noise operation that is required to discern the small amount of ionization that will be generated in a low-energy ion strike. This detection system has been primarily used for the construction of prototype solid-state quantum computer devices for Si:P architectures [2], but the ability to detect the response from an individual low-energy ion also opens the way to pursuing more fundamental tests on ion–solid interactions in this energy regime, which may be difficult to study by other methods. The device displayed in figure 1 is able to function as a low-noise ion detector that can collect the ionization signals generated by low-energy ions from within its central 10 μm × 10 μm active area, since this region contains a surface oxide layer of only 5 nm thickness. Previous characterization of these devices by a 2 MeV He^+ ion beam in a Nuclear Microprobe [3] has been used to test whether full charge collection of the

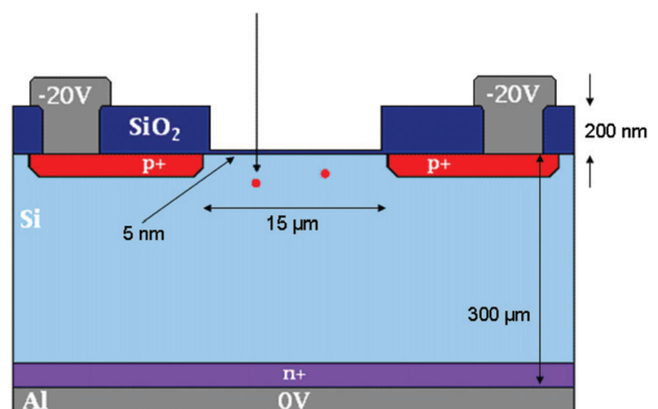

Figure 1. Schematic diagram of a single ion detector architecture integrated into a high-resistivity silicon wafer, based on a reverse-biased pin configuration. The detector contains a central 10 μm × 10 μm implantation region for counting low-energy ions.

 © 2008 IOP Publishing Ltd Printed in the UK

generated ionization is able to be achieved within the central active area of the detector structure. This was indeed found to be the case, with experiments showing that close to 100% of the generated signal from an ion strike was able to be collected by the detector before recombination occurred.

This structure therefore provides a way to directly investigate the properties of low-energy ion interactions with silicon, by measuring the ionization response generated in the detector substrate by individual ion events. To achieve this, a Colutron low-energy ion implanter [4] is utilized, which is able to generate a beam of ions of a number of different species. Before implantation, the silicon detector and its associated front-end electronics are both cooled by liquid nitrogen down to a temperature of 90 K, as measured by a thermistor, in order to minimize the electronic noise that will be present. By measurement of the ionization signal induced in the detector by single ions of varying energies and species, this system can then be used to both study the electronic stopping properties of such ion–solid interactions, as well as indirectly to investigate the nuclear stopping (i.e. damage) properties.

2. Ionization studies

When an incident ion penetrates a solid material, it will dissipate its initial energy through two separate interactions within the solid. The first of these is nuclear stopping, where atoms in the solid receive energy by elastic interactions with the incident ion, leading to recoils. Such collisions can involve the transfer of a significant amount of energy from the ion, and can also cause a large angular deflection of its trajectory. Furthermore, because the transfer of energy in these collisions goes into the movement of atoms away from their initial positions in the solid, it can also cause the creation of sites of lattice disorder, which usually manifests itself in the form of vacancy-interstitial defects [5] (also known as Frenkel Pairs). The other process by which an ion may dissipate energy as it traverses the solid, is in the creation of electron–hole pairs through the ionization of lattice atoms, also known as electronic stopping. Inelastic interaction of the ion with the electrons of atoms in the lattice can cause them to be either excited or else knocked out completely. Unlike in nuclear collisions, the individual interactions here will involve only a very small loss of the incident ion energy, as well as negligible deflection of its trajectory; and little or no vacancy creation will occur in the lattice.

These two stopping mechanisms will both act to govern the resultant behaviour of an ion travelling through a target material, including defining its range, straggling, and ionization generation. In order to calculate these parameters for various different incident ions and targets, researchers often turn to the semi-empirical Monte Carlo simulation code SRIM 2006 [6], which is widely used for the simulation of ion–solid interactions [7, 8]. SRIM utilizes the binary-collision approximation [9]—which describes the motion of particles by simulating sets of binary collisions between the particle and target atoms along its trajectory—to calculate values for the range and nuclear stopping of the incident ion. These binary collisions are screened Coulombic interactions, which are described in the code by the use of the ZBL universal repulsive potential developed by Ziegler *et al* [10].

To describe the electronic stopping power in the target is a more complicated problem. Since these collisions are inelastic, they may result in excitations of the electron cloud of the ion, and as such cannot simply be treated as a classical scattering problem between two charged particles. In the ion energy range above several hundred keV, the situation can be theoretically modelled to within an accuracy of a few per cent, based on the Bethe–Bloch formula [11, 12]. However, below around 100 keV amu^{-1} it becomes almost impossible to describe the electronic stopping power theoretically, and semi-empirical stopping models must instead be used. The most popular of these—and the one that is utilized in SRIM—is the so-called ZBL stopping model [10]. Recently, new attempts have been made to extend the theoretical range of electronic stopping power calculations towards lower energies [13, 14]; however, these models are still inaccurate at the very low energies (i.e. <5 keV amu^{-1}) that we intend to examine.

In fact, experimental measurements of the electronic stopping power of ions in such a low-energy regime—and hence their comparison with current theoretical models—have been surprisingly rare. Recently, however, Funsten *et al* have published a number of papers [15–17] in which experimental results have indicated that for ions implanted into silicon with a very low-energy (<2 keV amu^{-1}), SRIM will tend to greatly overestimate the total ionization created in the substrate. This implies that the electronic stopping power model utilized by SRIM is inadequate at such energies, a conclusion further strengthened by previous discrepancies associated with low keV amu^{-1} values, including the range of rare-earth elements in silicon and silicon dioxide [18], as well as in the electronic stopping power of gold ions in silicon [19].

The experimental studies that were undertaken by Funsten *et al* involved the use of pn junction-based silicon photodiodes, which contained a surface oxide layer just 6 nm thick. Tests previously carried out on these detectors with visible photons had shown that they were able to provide close to 100% charge collection efficiency for induced carriers, with negligible recombination of the carriers occurring within the silicon [20]. These devices were not operated in a single ion detection mode, but instead relied on a high beam current incident on the active area, in order to generate a large current signal within the photodiode due to ionization. By subtracting the detector's background leakage current from this induced photodiode current, and then dividing the result by the beam current itself (measured both pre- and post-implantation using a Faraday cup), the ionization response of the detector to single ions could thus indirectly be inferred.

This technique was used to characterize the response of various ion species and energies, down to a very low keV amu^{-1} value. The results of these measurements, plotting the ratio of the theoretical and experimental ionization responses, $f_{E,\mathrm{SRIM}}/f_E$ (where f_E represents the fraction of the ion's incident energy that will be lost to electronic stopping), against the scaled energy, $E/mZ^{1/2}$, of the incident ion, are shown in figure 2(a). These appear to demonstrate not only that there exists a large discrepancy between experiment and

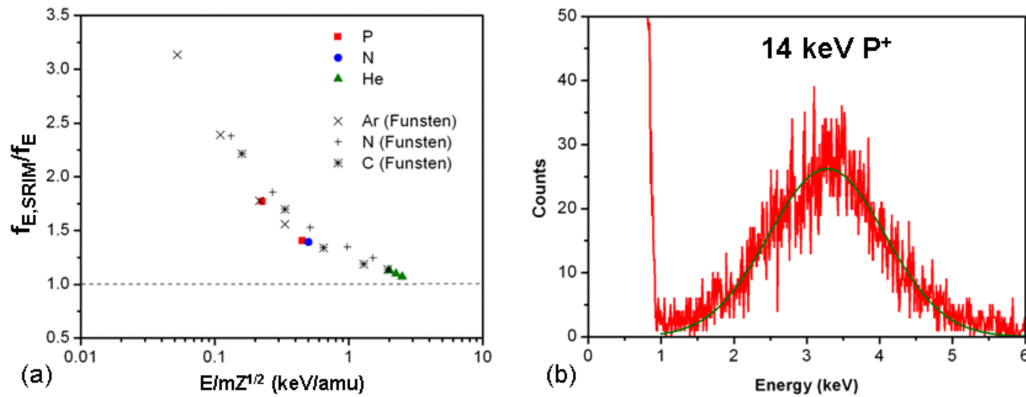

Figure 2. (a) Comparison of SRIM simulated ionization values with experimental data, measured using single ion detection. Previous results obtained by Funsten *et al* [15] for various species are also overlaid on this plot. (b) Ionization response obtained at 90 K from the implantation of 14 keV P^+ ions into a single ion detector.

theory at such low energies, but that this discrepancy also tends to increase rapidly with a decreasing incident ion energy. We wished to investigate whether the discrepancy reported in these results could be reproduced in our own system, using single ion detection. The disadvantage of this approach is that the direct detection of single ion events becomes challenging at low energies, largely due to the pulse-height defect [21, 22] which acts to divert much of the incident ion energy into avenues other than the generation of ionization (primarily to nuclear collisions within the substrate). This will therefore provide a limitation on the range of energies that we can probe using this technique; however, it will also potentially allow for more accurate results to be obtained than via photocurrent measurements.

In order to repeat these experiments by the direct measurement of the electronic stopping of low-energy ions in the keV regime, we chose three ion species of widely separated mass (He, N, and P), and measured the ionization response generated in our silicon detectors by the single ion events. A typical spectrum that resulted from these measurements—in this case for 14 keV P^+ ions—is shown in figure 2(b). In all of our measurements, the number of ions implanted into the detector active area was limited to a value low enough to avoid any potential decrease in the ionization signal due to damage effects, yet still high enough to be able to accurately determine the energy peak centroid. One potential concern when undertaking these experiments was that although the electron–hole pair creation energy is generally treated as a constant value, it is nevertheless predicted to have an energy dependence for very small incident energies [23], which could potentially affect the accuracy of our results. However, previous experimental measurements have shown that this effect will only begin to manifest itself at incident energies of less than 1 keV [24], and is therefore expected to be insignificant in the case of our experiments.

The results of our measurements are displayed in figure 2(a), with the previous results obtained by Funsten *et al* overlaid for comparison. It should be noted that SRIM does not take into account any possibility of ion channelling in the substrate, an effect which has the potential to affect the electronic stopping power of the ions; however, previous theoretical simulations of our devices [25] have shown that the surface oxide layer that is present will act to reduce channelling to negligible levels for the implant energies that we are utilizing. Our experimental data clearly agrees well with the previous results obtained by Funsten *et al*, with the magnitude of the discrepancy appearing to increase as an inverse function of the incident energy per unit mass. Interestingly, in the experiments of Funsten *et al*, the only ion species which did not follow the common trend was He, which only tended to manifest a discrepancy at a keV amu^{-1} value of 1 or below; a result that they had no explanation for [15]. In our measurements, however, it appears that He does show a discrepancy consistent with the rest of the ion species, even at higher energy. Future investigation of the behaviour of He ions over a wider ranger of energies would be useful, in order to potentially shed more light on this issue.

These results indicate that the current theoretical model used by SRIM to describe electronic stopping is largely inadequate in this low-energy regime. There are other potential theoretical approaches which can also be used to calculate electronic energy losses at low energies, including the LSS [26, 27] and Firsov [28] models. In fact, experimental results have tended to show that at sub-100 keV energies an LSS model will generally be more accurate in predicting electronic stopping than SRIM [29], although it will still tend to overestimate the percentage of incident energy that goes into creating ionization. A modified version of the LSS model proposed by Tilinin [30] fares better; by taking into account the correlation between electronic and nuclear collisions, the linear dependence of electronic energy loss on particle velocity is shown to be no longer valid at low energies, resulting in a model that reduces the electronic stopping power of ions in this regime. Even more promisingly, Akkerman and Barak have recently proposed a new theoretical model for low energies [31], which utilizes a binary-collision approach and combines elements of both the LSS and Firsov models by treating interactions as a mixture of local and non-local processes. This model has now been shown [32] to be able to provide a very good fit to the electronic stopping results measured by Funsten *et al* and confirmed in this work.

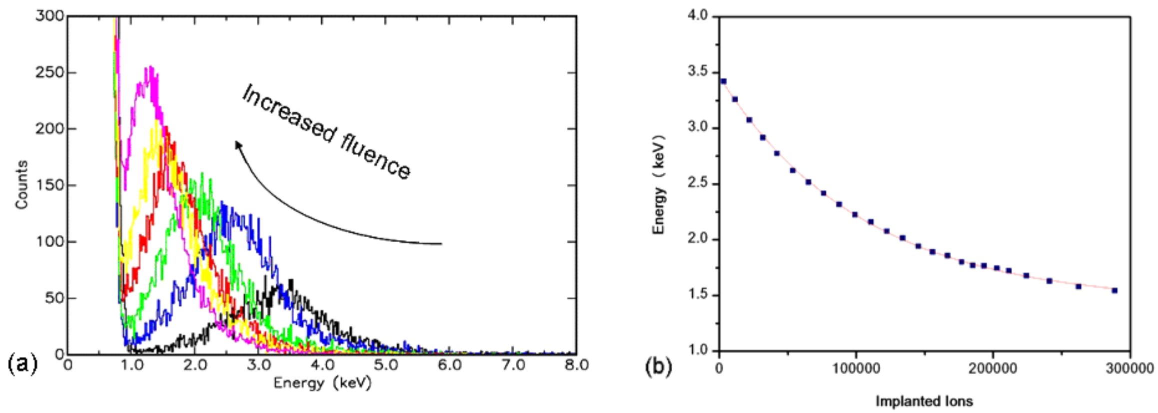

Figure 3. (a) A series of energy spectra, showing the change in the ionization response of a single ion detector as a function of the ion irradiation fluence, for a 14 keV P^+ implant at 90 K. The signal reaches saturation at a minimum ionization value of around 1.43 keV. (b) Plot of the average ionization response as a function of the ion fluence, based on Gaussian fits to the energy peaks in these spectra. The solid line represents an exponential fit performed on the data.

3. Damage studies

The ionization response of a detector can also be used to investigate the damage created by ion irradiation, as follows. The interaction of the incident ions with host atoms in the silicon will act to displace them from their lattice sites, generating defects in the silicon bandgap in the form of deep energy levels [33]. These recoiling atoms may themselves also create further displacements in the lattice, and by doing so introduce additional defect states. When charge carriers generated in the substrate then traverse an area that contains such defects, they may become trapped; and if the subsequent de-trapping of these carriers occurs on a timescale that is larger than the recombination time of the carriers themselves, this may then lead to a loss of some of the detected charge signal [34]. The nature of this defect creation process will be largely dependent on the species of the incident ion. Typically, light mass ions like boron will generate a number of small damage cascades spread out along the incident ion path, whereas a heavier ion like arsenic will tend to create a single large-scale cluster of disorder, centred on the ion track. In the case of these heavy ion interactions, if the irradiation is performed at a high enough fluence, these individual damage clusters will eventually begin to overlap, leading to the formation of a continuous amorphous layer.

During the ionization measurements undertaken in section 2, we subjected one detector to a sustained irradiation by 14 keV P^+ ions, and monitored the change in the detector's ionization response as a function of the ion fluence in the 10 μm $\times$ 10 μm implantation region. Some of the resultant experimental spectra obtained from this measurement are displayed in figure 3(a). What we found from this was that although the initial generated ionization was around 3.5 keV, this value began to decay immediately. As we continued to implant ions, the centroid of the energy peak underwent what appeared to be an exponential decrease. A plot of the ionization response as a function of the ion fluence was obtained by fitting Gaussian peaks to each of these spectra, the results of which can be seen in figure 3(b). An exponential could then be fitted to the decay curve, which indicates saturation of the signal at a baseline of around 1.43 keV.

The exponential decay of the energy signal, and its subsequent saturation to a non-zero value, both match previous experimental results obtained for silicon detectors operating at cryogenic temperatures [35]. These results had shown that the degradation in the signal was a function both of the ion fluence and of the applied reverse bias, with this latter factor influencing both the drop-off rate and the final saturation point of the ionization response. There are several potential explanations for the bias dependence of this saturation level: one is that the greater drift velocity associated with ions that are subject to a higher bias, would allow them to pass out of the damaged region in a shorter time, thus causing less charge to become trapped there (and hence lost). Alternatively, the amount of trapped charge may in fact be the same in each case, but nevertheless the reduction in the total drift time of charge to the back contact as a consequence of the larger applied bias, might still allow for a higher percentage of the charge to reach this point prior to the carrier recombination time.

With respect to the actual process that will govern this ionization degradation, the orthodox view of damage formation by a single heavy ion, as represented in the Gibbons overlap model [36], is that the impact will act to create a small core of either amorphized or else heavily damaged silicon in the region surrounding the ion track. In this model, the gradual amorphization of an ion implanted silicon layer will occur either by the process of direct amorphization of the areas around individual implantation locations, or else by the overlap of the damaged (but not amorphized) regions created by a number of ions, which will then act to form these amorphous zones. This process can be summarized in terms of an equation for the amorphous fraction, A_A, of the total implanted area (A_0):

$$A_A = A_0\left[1 - \left(\sum_{k=0}^{n} \frac{(A_i\Phi)^k}{k!}\exp(-A_i\Phi)\right)\right]. \qquad (1)$$

Here, A_i is the area of amorphous material produced by a single ion, Φ is the ion fluence, and n is the number of

overlapping damage tracks required to create an amorphous core. If $n = 0$, then each ion is capable of producing such a core simply by its own impact, and no overlap of the individual tracks will be required to amorphize the layer. In the case of a heavy ion impact, the amorphization process usually does not require any overlap of damaged regions, and at liquid nitrogen temperatures it has been shown that this will usually also be the case for lower mass ions as well [37]. The diameter of the amorphous core that will be formed in such an impact is dependent both on the ion species and energy, and for low-energy ions like ours, will generally be in the range of 0.5–2.5 nm at liquid nitrogen temperature [38].

If the $n = 0$ case is valid, then the damage process caused by ion implantation involves a series of statistically independent events, and the probability of creating further damage will be proportional to the undamaged area that remains in the implantation region. When making an indirect measurement of such a damage process—in this case, of the ionization response—it can be shown [39] that, as in equation (1), an exponential decay proportional both to the ion fluence and the value of A_i will then result. Since our experimental measurements correspond very well to an exponential decay, it can be assumed that the zeroth-order Gibbons model is indeed the correct description of the process, and that the build-up of damage in our devices is therefore occurring as a result of the individual ion strikes, rather than relying on the overlap of damage caused by multiple ion events. From this exponential decay, we can furthermore obtain the effective damage diameter of a single ion, which we calculate to be 34.8 ± 0.7 nm. Interestingly, this value is far larger than the diameter of the amorphous core that is expected to be created in such a single ion event, indicating that some other damage mechanism must also be occurring in the substrate.

There has been much work done on the amorphization of a silicon crystal, due to its applications in the semiconductor industry (i.e. for the reduction of ion channelling [40]), but the precise nature of the pre-amorphization damage that leads up to this point is still somewhat unclear [41]. The reason for this is that the formation of defects in the pre-amorphization stage is very hard to observe and requires high resolution transmission electron microscopy (TEM) [42]. Nevertheless, previous TEM studies on implanted silicon have reported that apart from the small characteristic amorphous core created in a single ion strike, there are also indications of an additional region of damage that extends outwards for 20–50 nm from the central impact point [43]. Subsequent diffraction contrast analysis on these regions have shown that they represent areas of fairly high disorder [44], but the exact nature of this disorder is still unclear, due to the limitations of the TEM technique [45].

The most likely explanation for these results, we propose, is that residual charge trapped in the core of the ion track could modify the silicon band structure in the vicinity of each ion strike and in doing so reduce the local electric field. This would then reduce the charge collection efficiency over a diameter of 40 nm, as has been inferred from the reduction of secondary emission efficiency from studies in diamond [46] over a similar radius. There may be other potential explanations for such an extended disorder profile, however: for example, it is well known that ion implantation into silicon can lead to the formation of internal stress fields due to the presence of the introduced dopants [47], and that the effects from this can extend out to significant distances. It has further been shown that the presence of such stresses can affect the nature of the damage that is created by ion implantation [48]. However, the mechanism by which these effects could lead to damage curve we observed is not clear.

Funsten *et al* also studied the issue of ion track damage radius [49], and by use of the detector architecture and technique that was described previously, obtained an effective damage diameter of around 35 nm for a 10 keV Ar ion impact, a value very similar to our own. A team at Waseda University also briefly investigated this question [50]. Their experiments involved irradiating Schottky diodes fabricated on n-type silicon of resistivity 1–2 Ω cm, and measuring the change in the series resistance as a function of the ion fluence. They found that the effective diameter of damage created by a single 75 keV Ar ion strike into silicon extended up to 21 nm. This is not quite as large as the diameter we observed, but that is unsurprising, since the incident energy was significantly higher. Also, these implantations were carried out at room temperature, meaning that many of the defects that were created may have subsequently self-annealed, due to the fact that at this temperature, single vacancies and interstitials are now mobile [51].

Since the Waseda result was based on measurement of the electrical, rather than the structural properties of silicon, it was capable of detecting effects caused by defect concentrations much lower than those that could be resolved in TEM studies. They were able to achieve a strong match of their experimental results to a theoretical model by postulating, as the previous TEM analysis had suggested, that the damage caused by a single ion in fact consisted of two separate regions: the small amorphous core, and a much larger zone of damage that surrounded it (figure 4). This latter region, with its much larger associated area, then appears to act as the dominant mechanism in altering the electrical properties of the silicon. Our experimental results seem to back up this model of damage accumulation, since they indicate that the damage generated by a single ion strike is not merely confined to the region of the small amorphous core known to be created by such events. However, since neither recoiling ions nor delta rays generated in collisions are expected to extend out as far as the diameters calculated in this and other studies indicate, we suggest that the residual charge trapped in the ion track core is responsible for the reduction in charge collection efficiency. Further work is required to characterize the interaction of ions with silicon in such a low-energy regime, in order to better understand the exact mechanism that governs the pre-amorphization disorder that is being produced in such cases.

4. Conclusion

In this paper, we have investigated ion–solid interactions in silicon in the low-energy regime, and compared the experimental results that were obtained to current theoretical models. By the use of a single ion detection technique,

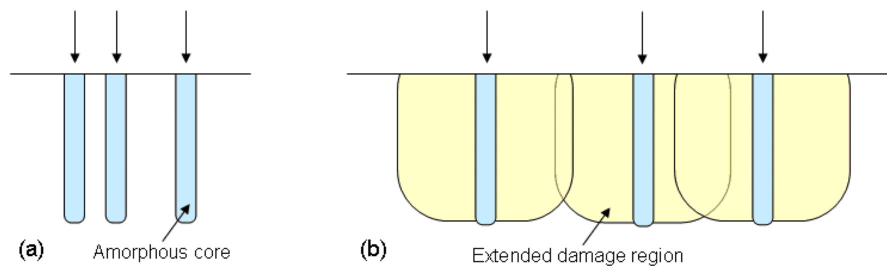

Figure 4. (a) The Gibbons model of damage formation in a semiconductor (zeroth order). The individual ion strikes generate small amorphous cores, which at high enough fluence, overlap to create a continuous amorphous layer. (b) Proposed alternative model of damage formation, whereby individual ion strikes also create a second broader region of damage, which extends out well beyond their amorphous cores.

we confirmed earlier reported results that indicated a large discrepancy between experiment and electronic stopping powers predicted by the SRIM code at energies below around 2 keV amu^{-1}; a result that indicates the use of more sophisticated theoretical models is required in this energy regime. Measurements of the fluence-dependent ionization response of a single ion detector to incident 14 keV P^+ ions, which yielded an effective damage diameter of 34.8 ± 0.7 nm for a single ion, then also led us to conclude that current models governing damage accumulation are inadequate, with the existence of an extended region of damage created by such events being proposed as a potential explanation for the measured data.

Acknowledgments

This work is supported by the Australian Research Council, the Australian Government and by the US National Security Agency (NSA), Advanced Research and Development Activity (ARDA) and the Army Research Office (ARO) under Contract Number DAAD19-01-1-0653. Financial support was also provided by the David Hay Memorial Fund. We are grateful to Alberto Cimmino for expert assistance with operation of our 14 keV implantation system, Eric Gauja for the skilled fabrication of the detectors we used in this study and to Andrew Dzurak and Steven Prawer for useful discussions.

References

[1] Jamieson D N, Yang C, Hopf T, Hearne S M, Pakes C I, Prawer S, Mitic M, Gauja E, Andresen S E, Hudson F E, Dzurak A S and Clark R G 2005 *Appl. Phys. Lett.* **86** 202101
[2] Hollenberg L C L, Dzurak A S, Wellard C, Hamilton A R, Reilly D J, Milburn G J and Clark R G 2004 *Phys. Rev.* B **69** 113301
[3] Yang C, Jamieson D N, Hearne S M, Pakes C I, Rout B, Gauja E, Dzurak A S and Clark R G 2002 *Nucl. Instrum. Methods* B **190** 212
[4] Colutron Research Corporation, Boulder, CO, http://www.colutron.com
[5] Tamura M 1991 *Mater. Sci. Rep.* **6** 141
[6] *SRIM—The Stopping and Range of Ions in Matter* http://www.srim.org
[7] Messenger S R, Burke E A, Summers G P, Xapsos M A and Walters R J 1999 *IEEE Trans. Nucl. Sci.* **46** 1595
[8] Randhawa G S and Virk H S 1996 *Radiat. Meas.* **26** 541
[9] Robinson M T and Torrens I M 1974 *Phys. Rev.* B **9** 5008
[10] Ziegler J F, Biersack J P and Littmark U 1996 *The Stopping and Range of Ions in Solids* (New York: Pergamon)
[11] Bethe H 1930 *Ann. Phys.* **5** 325
[12] Bloch F 1933 *Ann. Phys.* **16** 285
[13] Grande P L and Schiwietz G 2002 *Nucl. Instrum. Methods* B **195** 55–63
[14] Schinner A and Sigmund P 2002 *Nucl. Instrum. Methods* B **195** 64–90
[15] Funsten H O, Ritzau S M, Harper R W and Korde R 2001 *IEEE Trans. Nucl. Sci.* **48** 1785
[16] Funsten H O, Ritzau S M, Harper R W, Borovsky J E and Johnson R E 2004 *Phys. Rev. Lett.* **92** 213201
[17] Funsten H O, Ritzau S M, Harper R W and Korde R 2004 *Appl. Phys. Lett.* **84** 3552
[18] Palmetshofer L, Gritsch M and Hobler G 2001 *Mater. Sci. Eng.* B **81** 83
[19] Zhai Y J, Lu X T, Zheng T, Xia Z H and Shen D Y 1998 *Nucl. Instrum. Methods* B **135** 128
[20] Korde R and Geist J 1987 *Appl. Opt.* **26** 5284
[21] Britt H C and Wegner H E 1963 *Rev. Sci. Instrum.* **274** 34
[22] Ogihara M, Nagashima Y, Galster W and Mikumo T 1986 *Nucl. Instrum. Methods* A **251** 313–20
[23] Fraser G W, Abbey A F, Holland A, McCarthy K, Owens A and Wells A 1994 *Nucl. Instrum. Methods* A **350** 368–78
[24] Lechner P, Hartmann R, Soltau H and Strueder L 1996 *Nucl. Instrum. Methods* A **377** 206–8
[25] Wilson H F, Marks N A, McKenzie D R and Lee K H 2004 *Nucl. Instrum. Methods* B **215** 99
[26] Lindhard J, Nielsen V, Scharff M and Thomsen P V 1963 *Mat. Fys. Medd. Dan. Vidensk. Selsk.* **33** 1
[27] Lindhard J, Scharff M and Schiøtt H E 1963 *Mat. Fys. Medd. Dan. Vidensk. Selsk.* **33** 1
[28] Firsov O B 1959 *Sov. Phys.—JETP* **9** 1076
[29] Mangiarotti A, Lopes M I, Benabderrahmane M L, Chepel V, Lindote A, Pinta da Cunha J and Sona P 2007 *Nucl. Instrum. Methods* A **580** 114–7
[30] Tilinin I S 1995 *Phys. Rev.* A **51** 3058
[31] Akkerman A and Barak J 2006 *IEEE Trans. Nucl. Sci.* **53** 3667–74
[32] Akkerman A and Barak J 2007 *Nucl. Instrum. Methods* B **260** 529–36
[33] Kimerling L C 2003 *J. Appl. Phys.* **45** 1839
[34] Brodbeck T J, Chilingarov A, Sloan T, Fretwurst E, Kuhnke M and Lindstroem G 2000 *Nucl. Instrum. Methods* A **455** 645
[35] Borer K, Janos S, Palmieri V G, Dezille B, Li Z, Collins P, Niinikoski T O, Lourenco C, Sonderegger P and Borchi E 2000 *Nucl. Instrum. Methods* A **440** 5
[36] Gibbons J F 1972 *Proc. IEEE* **60** 1062
[37] Wang K W, Spitzer W G, Hubler G K and Sadana D K 1985 *J. Appl. Phys.* **58** 4553
[38] Dennis J R and Hale E B 1978 *J. Appl. Phys.* **49** 1119

[39] Fink D 2004 *Fundamentals of Ion-Irradiated Polymers* (Berlin: Springer)
[40] Pelaz L, Marques L A and Barbolla J 2004 *J. Appl. Phys.* **96** 5947
[41] Schreutelkamp R J, Custer J S, Liefting J R, Lu W X and Saris F W 1991 *Mater. Sci. Rep.* **6** 275
[42] Cellini C, Carnera A, Berti M, Gasparotto A, Steer D, Servidori M and Milita S 1995 *Nucl. Instrum. Methods* B **96** 227
[43] Ruault M O, Chaumont J and Bernas H 1983 *Nucl. Instrum. Methods* **209** 351
[44] Howe L M and Rainville M H 1987 *Nucl. Instrum. Methods* B **19** 61
[45] Ruault M O, Penisson J M, Chaumont J and Bourret A 1984 *Phil. Mag.* **50** 667
[46] Prawer S, Rubanov S, Hearne S M and Jamieson D N 2006 *Phys. Rev.* B **73** 153202
[47] Lee C S, Lee J H, Choi C A, No K and Wee D M 1999 *J. Micromech. Microeng.* **9** 252
[48] Mis J D, Mader S R and Beshers D N 1993 *J. Appl. Phys.* **74** 2294
[49] Ritzau S M, Funsten H O, Harper R W and Korde R 1998 *IEEE Trans. Nucl. Sci.* **45** 2820
[50] Koyama M, Cheong C W, Yokoyama K and Ohdomari I 1997 *Japan. J. Appl. Phys.* **36** L708
[51] Corbett J W, Karins J P and Tan T Y 1981 *Nucl. Instrum. Methods* **182** 457